Coexistence of type-I and type-II band alignment in Ga(Sb,P)/GaP heterostructures with pseudomorphic self-assembled quantum dots

D. S. Abramkin[+1)], *V. T. Shamirzaev*[*] *M. A. Putyato*[+], *A. K. Gutakovskii*[+], *T. S. Shamirzaev*[+×]

[+] *Rzhanov Institute of Semiconductor Physics SB of the RAS, 630090 Novosibirsk, Russia*

[*] *Novosibirsk State Technical University, 630092 Novosibirsk, Russia*

[×] *Novosibirsk State University, 630090 Novosibirsk, Russia*

Submitted 8 November 2013

Band alignment of heterostructures with pseudomorphic $GaSb_{1-x}P_x$/GaP self-assembled quantum dots (SAQDs) lying on wetting layer was studied. Coexistence of type-I and type-II band alignment was found within the same heterostructure. Wetting layer has band alignment of type-I with the lowest electronic state belonging to the X_{XY} valley of $GaSb_{1-x}P_x$ conduction band, in contrast to SAQDs, which have band alignment of type-II, independently of the ternary alloy composition x. It is shown that type-I – type-II transition is a result of GaP matrix deformation around the SAQD.

DOI: 10.7868/S0370274X14020040

Heterostructures with self-assembled quantum dots (SAQDs) are interesting for novel light-emitting device application [1]. The size-dependent emission of SAQDs allows one to fabricate light-emitting devices for a wide wavelength range. Up to date, the main attention has been devoted to SAQDs formed in GaAs matrix that emit in the near infrared spectral range, for example, (In,Ga)As/GaAs [2]. At the same time, SAQDs emitting in the visible wavelength range receive much less attention. Changing the GaAs matrix for a wide band-gap semiconductor provides a shift of SAQDs emission to the visible wavelength range. At present, the best-studied heterostructures are those formed in the wide-gap (Al,Ga)As matrix [3]. Nevertheless, Al-mediated defects result in reduced light-emitting efficiency [4–6]. The use of the GaP wide-gap matrix allows one to avoid the negative influence of Al-mediated defects and takes the advantage of well-developed Al-free light-emitting diode technology [7]. Recently, we have considered the atomic structure and band alignment of Ga(As,P) SAQDs and quantum well (QW) formed in GaP matrix [8, 9]. In the present report Ga(Sb,P)/GaP heterostructures are discussed. Since the lattice constants of GaSb and GaP are strongly mismatched (10.5% [10]), fully relaxed GaSb islands formed in Volmer–Weber growth mode on GaP surface have been solely studied [11–15]. In this letter we demonstrate the formation of the pseudomorphic Ga(Sb,P)/GaP SAQDs lying on wetting layer (WL). The band alignment of pseudomorphic Ga(Sb,P)/GaP SAQDs as well as WL is revealed. The coexistence of two different band structure types has been found.

The investigated structures were grown on the semi-insulator GaP (100)-oriented substrates by molecular beam epitaxy. The GaP buffer layer 160 nm thick was grown on the substrate at the temperature $T_S = 600\,^\circ$C. The deposition of GaSb was performed in the atomic layer epitaxy mode. The nominal amount of deposited GaSb equals to a bi-layer. The growth started with exposing to gallium for 10 s up to the formation of 1.0 monolayer Ga layer before any Sb deposition. Then, the Ga flux was turned off, and 1.0 monolayer of Sb was deposited. Two structures with SAQDs A and B were grown at $T_S = 420$ and $470\,^\circ$C, respectively. A capping 30-nm GaP layer was grown at the same T_S as the GaSb layer. Additionally, a test structure with the unstrained 30 nm GaP layer was grown in the same manner.

The investigation of the atomic structure and energy spectrum of SAQDs heterostructures was performed by means of transmission electron microscopy (TEM) and photoluminescence (PL) spectroscopy, together with computational work. TEM images were obtained using JEM-4000EX operated at 400 keV. Steady-state (*cw*) PL was excited by the GaN laser diode ($h\nu = 3.06$ eV), the excitation power density was varied within the range of 0.05–50 mW/cm^2 by a set of neutral optical filters. Time-resolved PL was excited by the third harmonic of Nd:YAG laser ($h\nu = 3.59$ eV) with the pulse duration of 5 ns and pulse energy density of 1 μJ/cm^2. The PL was analyzed with a spectrometer equipped with a

[1)] e-mail: demid@isp.nsc.ru

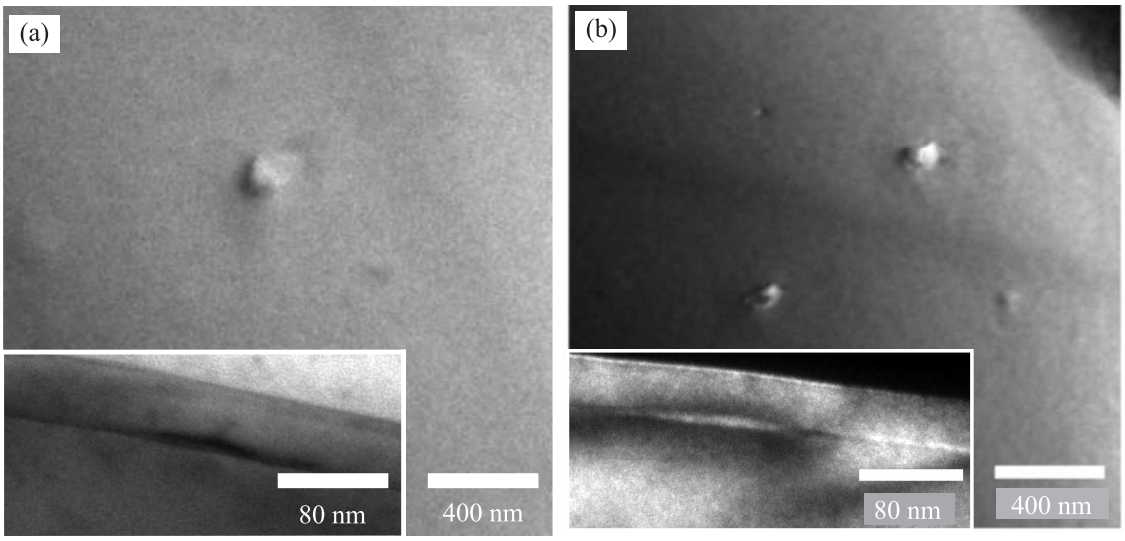

Fig. 1. TEM plan view and cross-section (in the inset) images of GaSb/GaP structures grown at 420 °C (a) and 470 °C (b), respectively

nitrogen-cooled CCD-camera for cw measurements and a cooled photomultiplier operated in the time-correlated photon-counting mode for time-resolved measurements. Calculation of $GaSb_{1-x}P_x$/GaP SAQDs and WL band alignment was performed using a Nextnano++ program package [16].

The plan view and cross-section TEM images of GaSb/GaP heterostructures with SAQDs grown at 420 and 470 °C are presented in Fig. 1a and b, respectively. One can clearly see that SAQDs are lying on WL in each structure. The thickness of wetting layer estimated from TEM images is of about 0.7–1.3 nm. The formation of the WL indicates that the SAQDs are formed in the Stranski–Krastanov growth mode independently of T_S. That is quite different from the Volmer–Weber growth mode for GaSb/GaP islands discussed in literature till now [11–14]. The SAQDs have lens-like shape with the aspect ratio of 1:10. The SAQDs height and diameter vary within the range of 8–12 and 80–120 nm, respectively. The SAQDs density is lower than $10^8\,cm^{-2}$. The main feature of the TEM images is pseudomorphic strain of the SAQDs. Since the GaSb/GaP heterosystem has a huge lattice mismatch, 10 the formation of large-sized and dislocation-free pseudomorphic SAQDs in the Stranski–Krastanov growth mode allows us to conclude that the SAQDs are not pure GaSb but consist of the ternary alloy $GaSb_{1-x}P_x$. We assume that the lateral diffusion of adatoms during SAQDs formation results in materials intermixing [17, 18], which leads to a reduction of SAQD/matrix lattice mismatch and the change in the growth mode.

Low-temperature (5 K) cw PL spectra of the $GaSb_{1-x}P_x$/GaP and test GaP/GaP structures measured at excitation power density (P_{ex}) of 50 mW/cm^2 are demonstrated in Fig. 2a. The spectrum of the test structure contains the bands at 1.40 and 2.20 eV, associated with impurity-related recombination in GaP [19, 20]. Additional PL bands with the intensity one-two orders of magnitude higher than that of the impurity-related PL bands appear in the spectra at 1.58 and 1.87 eV for structure A and 1.85 and 2.14 eV for structure B (marked in Fig. 2a as "QDs" and "WL", respectively). The low- and high-energy PL bands are connected with exciton recombination in quantum dots and wetting layer, respectively. The high PL efficiency at low P_{ex} evidences the quality of the studied heterostructures. The increase of the WL band intensity with increase in the growth temperature is a result of decrease in concentration of nonradiative centers in the WL and GaP matrix [21, 22].

Steady-state PL spectra of the $GaSb_{1-x}P_x$/GaP structures with SAQDs grown at 420 and 470 °C are presented in Fig. 2b and c, respectively, as a function of excitation power density within the range of 0.05–50 mW/cm^2. The blue shift of the QDs band is proportional to $P_{ex}^{1/3}$ as it is clearly shown in the upper insets of Fig. 2b and c. Deconvolution reveals that the WL bands consist of two bands with energy 1.87 and 1.92 eV for the structure A, and 2.13 and 2.17 eV for the structure B. Low-energy and high-energy bands connected with exciton recombination in ground and excited states, respectively. The increase of P_{ex} in 3 orders of magnitude

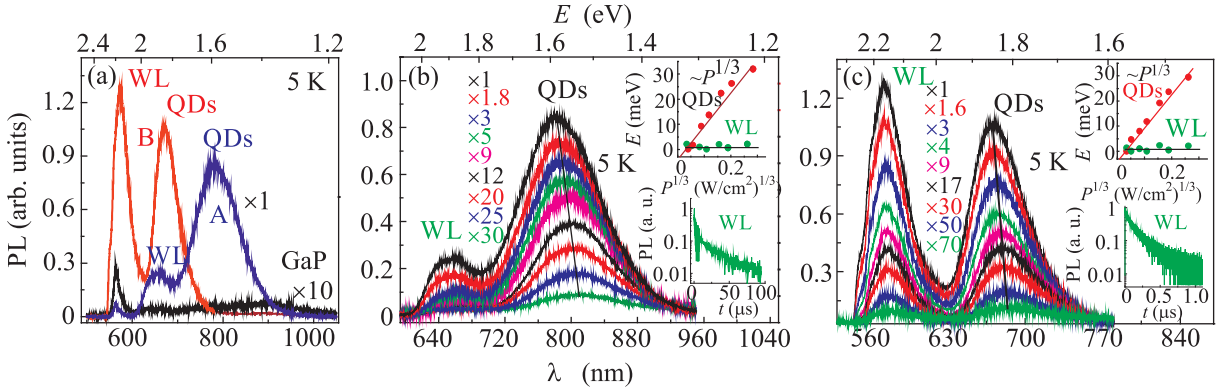

Fig. 2. (a) – Steady-state PL spectra of the A and B $GaSb_{1-x}P_x$/GaP structures and the test GaP/GaP structure, measured at $T = 5$ K and excitation power density of 50 mW/cm^2; Steady-state PL spectra of the structure A (b) and B (c), measured at $T = 5$ K and excitation power density P_{ex} changing within the range of 0.05–50 mW/cm^2. The upper insets show the PL bands energy position as a function of excitation power density. The dynamics of WL exciton photoluminescence measured at $T = 5$ K is shown in the lower insets

does not result in any spectral shifts of these PL bands. Saturation of the ground states population with increasing of excitation power density leads to increase in relative intensity of the high-energy bands. As a results WL band are distorted that manifested as a weak blue shift.

The blue shift proportional to $P_{ex}^{1/3}$ allows us to unambiguously define the band alignment of type-II for the SAQDs [23, 24]. On the other hand, we can conclude that the WL have the band alignment of type-I. Thus, the coexistence of two different types of energy spectrum is detected: $GaSb_{1-x}P_x$/GaP SAQDs have band alignment of type-II, while $GaSb_{1-x}P_x$/GaP WL has band alignment of type-I. It is necessary to note that despite the spatial localization of electrons and holes in the wetting layer, the WL band demonstrates a long (about 100 μs for structure A and about 1 ms for structure B) decay as it is shown in the bottom insets of Fig. 2b and c. An acceleration of WL PL decay with changing of T_S from 470 to 420 °C, as well as quenching of *cw* WL PL intensity, is ruled by increase of defect concentration in the WL and GaP matrix. A long PL decay in heterostructures with band alignment of type-I points to optical transition indirect in the momentum space as it was demonstrated in our recent studies [25–27].

In order to clarify the reason of the difference in the $GaSb_{1-x}P_x$/GaP SAQDs and WL band alignment, their energy spectra were calculated as a function of ternary alloy composition x. Band-structure parameters for the ternary alloy were determined by a linear approximation between GaSb and GaP parameters presented in [10, 28, 29]. Elastic strain for the SAQD and WL was calculated via elastic energy minimization [16]. Lattice constants for unstrained materials were taken in [10]. We took into account the strain effect on the band alignment by using macroscopic theory of elasticity: (i) change of band gaps due to change in the unit cell volume and (ii) splitting of the degenerate valence bands and of the degenerate indirect X minima in the conduction band induced by the biaxial component of the strain [30]. The technique of calculation was described previously in [25], 31]. The energy levels of electrons and holes were calculated in the simple band effective mass approach [26]. The WL thickness (0.7–1.3 nm) and the SAQDs size (height and diameter of 8–12 and 80–120 nm, respectively, with aspect ratio 1:10) were taken from the TEM data. Strain distribution in heterostructures is determinated by geometry factor. Since the WL is an ultra-thin quantum well, it is modeled as a pseudomorphic $GaSb_{1-x}P_x$ slab. The strain is fully localized within the $GaSb_{1-x}P_x$ layer in this configuration (two-dimensional strain distribution occurs), since the slab is matched with GaP matrix in the growth plane as it is shown in Ref. [32]. On the other hand, three-dimensional strain distribution takes place for lens-like shape of SAQD [33]. Thus, GaP matrix is deformed around the $GaSb_{1-x}P_x$ SAQD. For the sake of simplicity, the Coulomb interaction between electron and hole (exciton effect) was neglected.

The band edges and ground energy levels for electron and heavy holes in WL of 1 nm thickness, calculated as a function of alloy composition x, are presented in Fig. 3a. One can see that the $GaSb_{1-x}P_x$/GaP WL has band alignment of type-I and indirect band-gap with electron belonging to the X_{XY} valley of conduction band independently of ternary alloy composition x. In order to check robustness of this result we calculate energy spectrum of WL with thickness in range from 0.6 (cor-

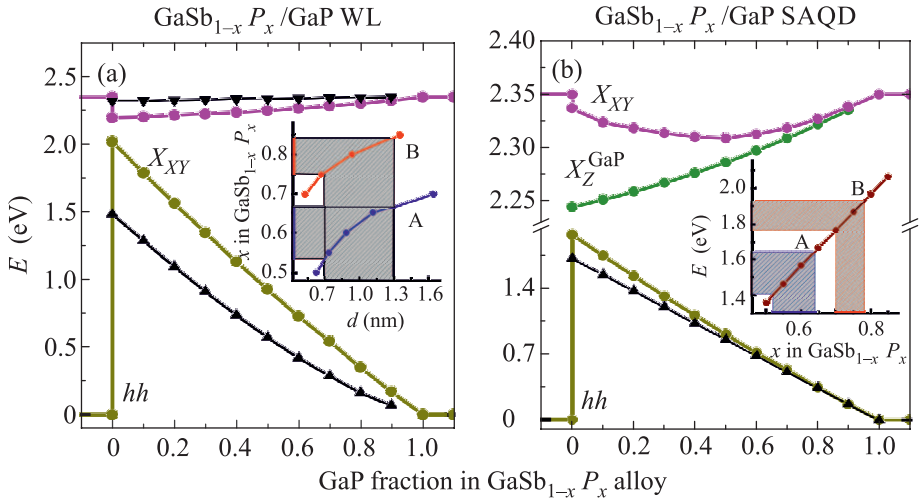

Fig. 3. Band edges (circles) and ground energy levels of electron and hole (triangles) as a function of ternary alloy composition x for: GaSb1 $-$ xP$_x$/GaP WL (a) and GaSb1 $-$ xP$_x$/GaP SAQD (b). The values of d and x corresponded to the optical transition energy of 1.87 and 2.13 eV (marked as "A" and "B", respectively) are shown in the insert to Fig. a. The optical transition energy for SAQDs as a function of x is shown in the insert to Fig. b. "A" and "B" mark change in composition x corresponds to change in optical transition energy within QDs bandwidth for heterostructure A and B, respectively

respond to one monolayer of GaSb) to 2 nm. Change in the thickness leads to shift of electron and hole energy levels however do not change the type of WL band alignment.

Band lineups calculated for the SAQD is presented in Fig. 3b. In this case, the biaxial strain of the matrix (having the opposite sign to the strain in SAQD) splits the states of the X valley of the GaP conduction band, the energy of the X_{XY} states increases and that of X$_Z$ decreases with respect to their unperturbed position. As a result, SAQD has band alignment of type-II, since the energy of matrix X_Z states lies below that of X_{XY} states of SAQD, independently of ternary alloy composition x. Due to weak quantum confinement a variation of the SAQD height in the range of 8–12 nm results in a weak shift of optical transition energy (about 10 meV) and not change the type of the band alignment.

A comparison of the PL emission energy with the energy of calculated optical transitions allows us to estimate the ternary alloy composition x in the WL and SAQDs. For thin WL energy of optical transition is controlled not only by alloy composition x but also by thickness of WL (d). The inset to Fig. 3a shows sets of values d and x corresponded to energy of optical transition equaled to 1.87 eV (structure A) and 2.13 eV (structure B), respectively. Taking into account uncertainty in the WL thickness (0.7–1.3 nm) we estimate the alloy composition x as 0.54–0.67 and 0.75–0.84 for WL formed at 420 and 470 °C, respectively. Band lineups corresponded to GaSb$_{0.2}$P$_{0.8}$/GaP WL is presented in Fig. 4a. The case of the SAQDs is essentially different. Since the SAQD height variation has weak effect on energy of optical transition that is controlled by ternary alloy composition x. Thus, the peak position and bandwidth of the QDs band is mainly ruled by dispersion in the alloy composition. The energy of optical transition for SAQDs of 10 nm height as function of x is presented in the inset to Fig. 3b. Taking into account parameters of the QDs bands we estimate dispersion in alloy composition x of the SAQDs as 0.52–0.64 and 0.70–0.78 for the A and B heterostructures, respectively. Band lineups corresponded to GaSb$_{0.25}$P$_{0.75}$/GaP SAQD is presented in Fig. 4b.

One can see that increasing of T_S leads to increase in the GaP fraction inside WL and SAQDs. There are two possible reasons for temperature dependence of WL and SAQDs composition. On the one hand, GaSb and GaP can be intermixed during surface interdiffusion similar to GaAs and GaP intermixing discussed in Ref. [9]. On the other hand, GaSb and GaP can be intermixed during growth of GaP capping layer by Sb segregation. Indeed, Sb atom has the largest radius among P, As, and Sb [34]. As a result, strong segregation of Sb occurs in III–V and VI semiconductors [35, 36] and the composition of buried SAQDs and WL can be differ drastically from that during the process of SAQDs formation. The determination of intermixing mechanisms is out of the framework of our study.

It needs to note that the driving force of the transition from two-dimensional to three-dimensional growth

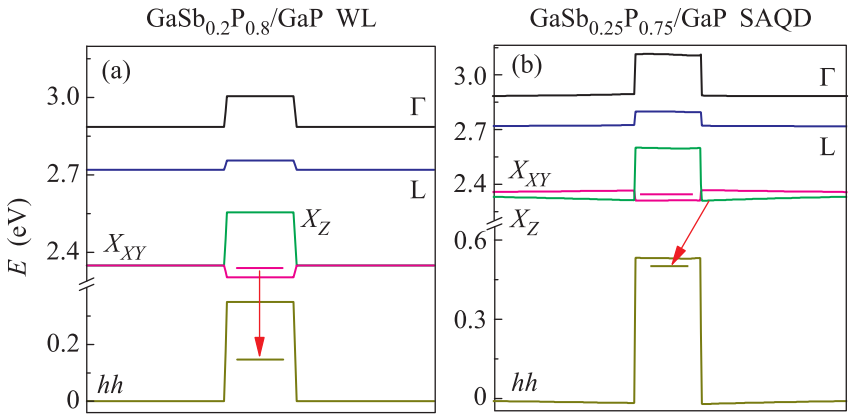

Fig. 4. Band lineups calculated for $GaSb_{0.2}P_{0.8}/GaP$ WL (a) and $GaSb_{0.25}P_{0.75}/GaP$ SAQD (b)

mode (2D–3D transition) of heteroepitaxial systems in Stranski–Krastanov mode is relaxation of the elastic energy of strained layer through the islands nucleation. The elastic energy depends on the lattice mismatch between the GaSbP (that formed SAQDs) and the substrate (GaP), whereas lattice mismatch between SAQDs and WL materials do not affect on dots formation.

In conclusion, pseudomorphic SAQDs in GaSb/GaP heterosystem were formed in the Stranski–Krastanov growth mode. The SAQDs consist of the ternary alloy $GaSb_{1-x}P_x$ as a result of materials intermixing during their formation. The energy spectra of wetting layer and quantum dots have been determined. $GaSb_{1-x}P_x/GaP$ WL has band alignment of type-I with the lowest electron state belonging to the X_{XY} valley of $GaSb_{1-x}P_x$ conduction band, while $GaSb_{1-x}P_x/GaP$ SAQDs have band alignment of type-II and the lowest electron state belonging to the X_Z valley of GaP conduction band for any value of ternary alloy composition $0 < x < 1$. Thus, the coexistence of two different types of band alignment in the same heterostructure has been revealed. The change of the SAQDs band alignment in comparison with that of the WL is explained by splitting the X valley of GaP conduction band due to the deformation of GaP matrix around the SAQD.

This work was supported by the Russian Foundation for Basic Research (Projects # 13-02-00073, 14-02-00033 and 14-02-31102), the Dynasty Foundation, The Russian Presidential Grant # SP-985.2013.5, and the Programs of the Ministry of Education and Science of Russian Federation (contract 16.552.11.7091).

1. Z. M. Wang, *Self-assembled Quantum Dots*, Springer, N.Y. (2008).
2. M. Grundmann, O. Stier, and D. Bimberg, Phys. Rev. B **52**, 11969 (1995).
3. K. Posilovic, T. Kettler, V. A. Shchukin, N. N. Ledentsov, U. W. Pohl, D. Bimberg, J. Fricke, A. Ginolas, G. Erbert, G. Trankle, J. Jonsson, and M. Weyers, Appl. Phys. Lett. **93**, 221102 (2008).
4. F. Bosc, J. Sicart, and J. L. Robert, J. Appl. Phys. **85**, 6520 (1999).
5. F. Bosc, J. Sicart, J. L. Robert, and R. Piotrzkowski, J. Appl. Phys. **88**, 1515 (2000).
6. R. Khlil, A. El Hdiy, and Y. Jin, J. Appl. Phys. **98**, 093709 (2005).
7. F. Hatami, V. Lordi, J. S. Harris, H. Kostial, and W. T. Masselink, J.Appl. Phys. **97**, 096106 (2005).
8. T. S. Shamirzaev, D. S. Abramkin, A. K. Gutakovskii, and A. Putyato, Appl. Phys. Lett. **97**, 023108 (2010).
9. D. S. Abramkin, M. A. Putyato, S. A. Budennyy, A. K. Gutakovskii, B. R. Semyagin, V. V. Preobrazhenskii, O. F. Kolomys, V. V. Strelchuk, and T. S. Shamirzaev, J. Appl. Phys. **112**, 083713 (2012).
10. I. Vurgaftman, J. R. Meyer, and L. R. Ram-Mohan, J. Appl. Phys. **89**, 5815 (2001).
11. S. El Kazzi, L. Desplanque, C. Coinon, Y. Wang, P. Ruterana, and X. Wallart, Appl. Phys. Lett. **97**, 192111 (2010).
12. Y. Wang, P. Ruterana, H. P. Lei, J. Chen, S. Kret, S. El Kazzi, L. Desplanque, and X. Wallart, J. Appl. Phys. **110**, 043509 (2011).
13. Y. Wang, P. Ruterana, J. Chen, L. Desplanque, S. El Kazzi, and X. Wallart, J. Phys.: Condens. Matter. **24**, 335802 (2012).
14. S. El Kazzi, L. Desplanque, X. Wallart, Y. Wang, and P. Ruterana, J. Appl. Phys. **111**, 123506 (2012).
15. D. S. Abramkin, M. A. Putyato, A. K. Gutakovskii, B. R. Semyagin, V. V. Preobrazhenskii, and T. S. Shamirzaev, Semicondutors **46**, 1536 (2012).
16. P. Vogl, T. Andlauer, A Trellakis, T. Zibold, P. Greck, T. Eissfeller, and S. Birner, *Nextnano++* (a program package).

17. Y. Tu, and J. Tersoff, Phys. Rev. Lett. **98**, 096103 (2007).
18. G. Katsaros, A. Rastelli, M. Stoffel, G. Isella, H. von Kanel, A. M. Bittner, J. Tersoff, U. Denker, O.G. Schmidt, G. Costantini, and K. Kern, Surf. Sci. **600**, 2608 (2006).
19. A. T. Vink, A. J. Bosman, J. A. van der Does de Bye, and R. C. Peters, Solid State Commun. **7**, 1475 (1969).
20. J. S. Jayson, R. Z. Bachrach, P. D. Dapkus, and N. E. Schumaker, Phys. Rev. B **6**, 2357 (1972).
21. J. H. Kim, H. Asahi, K. Asami, K. Iwata, S. G. Kim, and S. Gonda, Appl. Surf. Science **82**, 76 (1994).
22. T. K. Sharma, V. K. Dixit, T. Ganguli, S. D. Singh, S. Porwal, R. Kumar, P. Tiwari, and A. K. Nath, Semicond. Sci. Technol. **23**, 075031 (2008).
23. N. N. Ledentsov, J. Bohrer, M. Beer, F. Heinrichsdorff, M. Grundmann, D. Bimberg, S. V. Ivanov, B. Y. Meltser, S. V. Shaposhnikov, I. N. Yassievich, N. N. Faleev, P. S. Kopev, and Z. I. Alferov, Phys. Rev. B **52**, 14058 (1995).
24. F. Hatami, N. N. Ledentsov, M. Grundmann, J. Bohrer, F. Heinrichsdorff, M. Beer, D. Bimberg, S. S. Ruvimov, P. Werner, U. Gosele, J. Heydenreich, U. Richter, S. V. Ivanov, B. Ya. Meltser, P. S. Kop'ev, and Zh. I. Alferov, Appl. Phys. Lett. **67**, 656 (1995).
25. T. S. Shamirzaev, A. M. Gilinsky, A. K. Kalagin, A. V. Nenashev, and K. S. Zhuravlev, Phys. Rev. B. **76**, 155309 (2007).
26. T. S. Shamirzaev, A. V. Nenashev, A. K. Gutakovskii, A. K. Kalagin, K. S. Zhuravlev, M. Larsson, and P. O. Holtz, Phys. Rev. B **78**, 085323 (2008).
27. T. S. Shamirzaev, J. Debus, D. S. Abramkin, D. Dunker, D. R. Yakovlev, D. V. Dmitriev, A. K. Gutakovskii, L. S. Braginsky, K. S. Zhuravlev, and M. Bayer, Phys. Rev. B **84**, 155318 (2011).
28. S. H. Wei and A. Zunger, Phys. Rev. B **60**, 5404 (1999).
29. M. C. Munoz and G. Armelles, Phys. Rev. B **48**, 2839 (1993).
30. C. G. Van de Walle, Phys. Rev. B **39**, 1871 (1989).
31. T. S. Shamirzaev, Semiconductors **45**, 96 (2011).
32. M. Grundmann, O. Stier, and D. Bimberg, Phys. Rev. B **52**, 11969 (1995).
33. A. Schliwa, M. Winkelnkemper, and D. Bimberg, Phys. Rev. B **76**, 205324 (2007).
34. J. C. Slater, J. Chem. Phys. **41**, 3199 (1964).
35. J. F. Nutzel and G. Abstreiter, Phys. Rev. B **53**, 13551 (1996).
36. X. Wallart, S. Godey, Y. Douvry, and L. Desplanque, Appl. Phys. Lett. **93**, 123119 (2008).